

Targeted suicide gene therapy for liver cancer based on ribozyme-mediated RNA replacement through post-transcriptional regulation

Seung Ryul Han,^{1,7} Chang Ho Lee,^{2,7} Ji Young Im,² Ju Hyun Kim,² Ji Hyun Kim,¹ Sung Jin Kim,² Young Woo Cho,^{3,4} Eunkyung Kim,^{3,4} Youngah Kim,³ Ji-Ho Ryu,^{3,4} Mi Ha Ju,⁵ Jin Sook Jeong,⁵ and Seong-Wook Lee^{1,2}

¹R&D Center, Rznomics, Inc., Seongnam 13486, Republic of Korea; ²Department of Life Convergence, Research Institute of Advanced Omics, Dankook University, Yongin 16890, Republic of Korea; ³New Drug Development Center, Osong Medical Innovation Foundation, Cheongju 28160, Republic of Korea; ⁴College of Pharmacy, Chungbuk National University, Cheongju 28644, Republic of Korea; ⁵Department of Pathology and Immune-network Pioneer Research Center, Dong-A University College of Medicine, Busan 602-714, Republic of Korea

Hepatocellular carcinoma (HCC) has high fatality rate and limited therapeutic options. Here, we propose a new anti-HCC approach with high cancer-selectivity and efficient anti-cancer effects, based on adenovirus-mediated *Tetrahymena* group I *trans*-splicing ribozymes specifically inducing targeted suicide gene activity through HCC-specific replacement of telomerase reverse transcriptase (TERT) RNA. To confer potent anti-HCC effects and minimize hepatotoxicity, we constructed post-transcriptionally enhanced ribozyme constructs coupled with splicing donor and acceptor site and woodchuck hepatitis virus post-transcriptional regulatory element under the control of microRNA-122a (miR-122a). Adenovirus encoding post-transcriptionally enhanced ribozyme improved *trans*-splicing reaction and decreased human TERT (hTERT) RNA level, efficiently and selectively retarding hTERT-positive liver cancers. Adenovirus encoding miR-122a-regulated ribozyme caused selective liver cancer cytotoxicity, the efficiency of which depended on ribozyme expression level relative to miR-122a level. Systemic administration of adenovirus encoding the post-transcriptionally enhanced and miR-regulated ribozyme caused efficient anti-cancer effects at a single dose of low titers and least hepatotoxicity in intrahepatic multifocal HCC mouse xenografts. Minimal liver toxicity, tissue distribution, and clearance pattern of the recombinant adenovirus were observed in normal animals administered either systemically or via the hepatic artery. Post-transcriptionally regulated RNA replacement strategy mediated by a cancer-specific ribozyme provides a clinically relevant, safe, and efficient strategy for HCC treatment.

poorly to conventional therapy and frequently relapses after both surgical and nonsurgical treatments.³ Moreover, HCC-related incidence and mortality continue to increase in many countries and the majority of HCC patients are at an advanced stage with multifocal tumors, vascular invasion, and/or intrahepatic metastasis,⁴ which collectively have very limited therapeutic options. Kinase and immune checkpoint inhibitors have been US Food and Drug Administration (FDA)-approved as primary or secondary treatment options in HCC patients with the advanced stage cancer.² However, due to their limited indications, role in causing liver failure, low response rate, side effects, and resistance to the agents, they have limited utility for HCC. Therefore, there still exists an urgent need for new strategies to treat HCC. Genetic therapy has been explored as a new therapeutic approach that promises efficacy, cancer-selectivity, and safety, and would be a welcome addition to overcome current clinical shortcomings.⁵ However, there are high challenges to achieving its idealization.

We developed a *Tetrahymena* group I intron-based *trans*-splicing ribozyme, targeting human telomerase reverse transcriptase (hTERT) RNA and demonstrated that the adenovirus-mediated delivery of the ribozyme could efficiently induce activity of the suicide gene (herpes simplex virus thymidine kinase [HSVtk]) through target-specific RNA replacement.^{6–11} This occurred not only in cells, but also in tumor xenografts models when treated with pro-drugs. We observed that expression of the ribozyme under the control of liver tissue-specific promoter phosphoenolpyruvate carboxykinase (PEPCK)

INTRODUCTION

Hepatocellular carcinoma (HCC) accounts for more than 80% of primary liver cancers¹ and ranks as the fourth most common cause of cancer-related death worldwide.² Local ablation, surgical resection, or liver transplantation are used for the treatment of early-stage HCC patients and catheter-based locoregional treatment is applied for those with intermediate-stage HCC. However, HCC responds

Received 13 August 2020; accepted 24 October 2020;
<https://doi.org/10.1016/j.omtn.2020.10.036>.

⁷These authors contributed equally

Correspondence: Seong-Wook Lee, R&D Center, Rznomics, Inc., Seongnam 13486 and Department of Life Convergence, Dankook University, Yongin 16890, Republic of Korea.

E-mail: swl0208@rznomics.com; swl0208@dankook.ac.kr

Correspondence: Jin Sook Jeong, Department of Pathology and Immune-network Pioneer Research Center, Dong-A University College of Medicine, Busan 602-714, Republic of Korea.

E-mail: jsjung1@dau.ac.kr



conferred liver tissue specificity of the ribozyme activity, inducing anti-HCC effects without impacting normal liver tissue in intraperitoneal carcinomatosis HCC mouse xenografts.⁹ However, clinical translation using the tissue-specific promoter-mediated expression of ribozyme has been hampered due to its poor expression efficacy, thus requiring high dose of delivery vehicles including viral vector, which can induce toxicity and/or innate immunity.¹² In addition, this therapeutic approach to targeting hTERT for HCC may be limited due to the presence of normal proliferative liver cells of HCC patients with cirrhosis, which express low levels of hTERT during the premalignant or later stages of hepatocarcinogenesis¹³ and thus could also be targeted. Therefore, an approach that efficiently and specifically targets HCC hTERT RNA would be needed for the successful clinical translation of the ribozyme.

In this study, we developed a new *trans*-splicing ribozyme system harboring efficient antitumor effects with low amounts of delivery vehicle that simultaneously confers HCC-selectivity while causing minimal toxicity in normal liver. Previously, we showed that intracellular ribozyme expression level is a major determining factor for the *in vivo* efficacy of the ribozyme.¹⁴ In this study, we tested whether post-transcriptional enhancement of the intracellular expression level of the ribozyme, while maintaining promoter activity, could improve the *in vivo* ribozyme efficacy and thus lead to reductions in the viral titers delivered. To this end, we inserted post-transcriptional enhancer elements such as a splicing donor/acceptor (SD/SA) site, which controls RNA polymerase processivity, RNA processing, polyadenylation, and mRNA export.^{15–17} We also tested insertion of the woodchuck hepatitis virus post-transcriptional regulatory element (WPRE), which regulates expression by polyadenylation, mRNA export, or translation,^{18–21} into the hTERT-targeting ribozyme construct. Moreover, we found that incorporation into the ribozyme construct of target sites for normal liver-specific microRNA-122a (miR-122a)²² induced the miR-122a-regulated expression, and thus anti-HCC effects with minimal hepatotoxicity in intrahepatic multifocal HCC mouse xenografts.¹¹

In sum, we constructed post-transcriptionally enhanced and/or miR-122a-regulated *trans*-splicing ribozyme systems and evaluated their cellular and *in vivo* efficacy and safety as a tool for targeted HCC gene therapy. The aim was to address both the anti-cancer efficacy and the cancer-selectivity challenges raised by the TERT-targeting approach. Viral vectors encoding the ribozymes were constructed herein, and their target RNA specificity, transgene controllability, tissue selectivity, liver toxicity, and anti-cancer efficacy were analyzed in intrahepatic multifocal HCC mouse xenograft models. Moreover, liver toxicity and bio-distribution of the virus were assessed in normal animals.

RESULTS

Improved cytotoxicity toward cancer cells by adenovirus harboring the post-transcriptionally enhanced *trans*-splicing ribozymes

To enhance the intracellular expression of *trans*-splicing ribozyme, we inserted post-transcriptional elements into the previously described hTERT-targeting ribozyme expression vector under the

control of SV40 promoter (SRF)⁶ (Figure S1A). To this end, SD/SA or SD/SA (Δ 61-mer), the deleted mutant form of SD/SA, was inserted downstream of SV40 promoter. WPRE or WPRE reverse was inserted downstream of the 3' exon transgene of the ribozyme, firefly luciferase. In hTERT-positive cells, luciferase transgene activity by the enhanced *trans*-splicing ribozymes was increased approximately 2- to 8-fold, compared with control unmodified ribozyme SRF (Figure S1B). However, enhanced ribozymes did not increase the expression of transgene in hTERT-negative IMR90 cells (Figure S1C). Noticeably, enhanced ribozyme harboring both SD/SA and WPRE exhibited higher induction of transgene than other ribozymes in most hTERT-positive cells. This result indicated that post-transcriptional modification of the ribozyme construct with SD/SA and/or WPRE could significantly increase the target RNA-specific expression of transgene.

To test the anti-cancer effects of the enhanced ribozymes in cells, we constructed recombinant adenovirus delivery systems harboring the modified ribozyme construct with HSVtk as a therapeutic transgene (Figure 1A), and then compared their cytotoxicity with ganciclovir (GCV) treatment in hTERT-positive cancer cells. The enhanced ribozyme constructs with PEPCK promoter more efficiently reduced cell viability in HepG2 cells than the previously described liver-specific PEPCK promoter-driven hTERT-targeting ribozyme (Ad-PRT)⁹ (Figure 1B). Enhanced ribozyme constructs with cytomegalovirus (CMV) promoter also improved cytotoxicity on both Hep3B and HT29 cells, compared with the previously described CMV promoter-driven hTERT-targeting ribozyme (Ad-CRT)⁶ (Figure 1C). The results indicated that post-transcriptional modification of the ribozyme construct with SD/SA and/or WPRE sites could significantly increase the cytotoxicity toward cancer cells irrespectively of promoter types.

To determine whether the increase in cell death activity by the modified ribozyme adenoviral vectors occurred through enhanced *trans*-splicing reaction, we performed RNase protection assay (RPA) in hTERT-positive Hep3B cells (Figure 1D). To this end, we generated radiolabeled RNA probes for the detection of *trans*-splicing molecules (TSM) of hTERT-targeting ribozymes. The experiment was designed so that three bands of different sizes representing target hTERT RNA, HSVtk RNA, or TSM could be produced through RPA with the probe if the *trans*-splicing reaction occurred (Figure S2). *Trans*-splicing products were specifically detected by adenoviruses encoding the ribozyme, but not by either control adenovirus encoding luciferase (CL) or HSVtk (CT; Figure 1D). Of note, TSM was observed more with adenoviruses harboring enhanced ribozyme constructs than unmodified Ad-CRT. In particular, adenovirus harboring both SD/SA and WPRE (Ad-SD/SA CRT WPRE) most efficiently induced the *trans*-splicing reaction. Accordingly, the level of target hTERT RNA was more drastically reduced by adenoviruses harboring the enhanced elements and Ad-SD/SA CRT WPRE reduced hTERT RNA most efficiently. These results suggested that increased cell death activity by the modified ribozyme adenoviral vectors occurred through enhanced *trans*-splicing reaction and simultaneous target

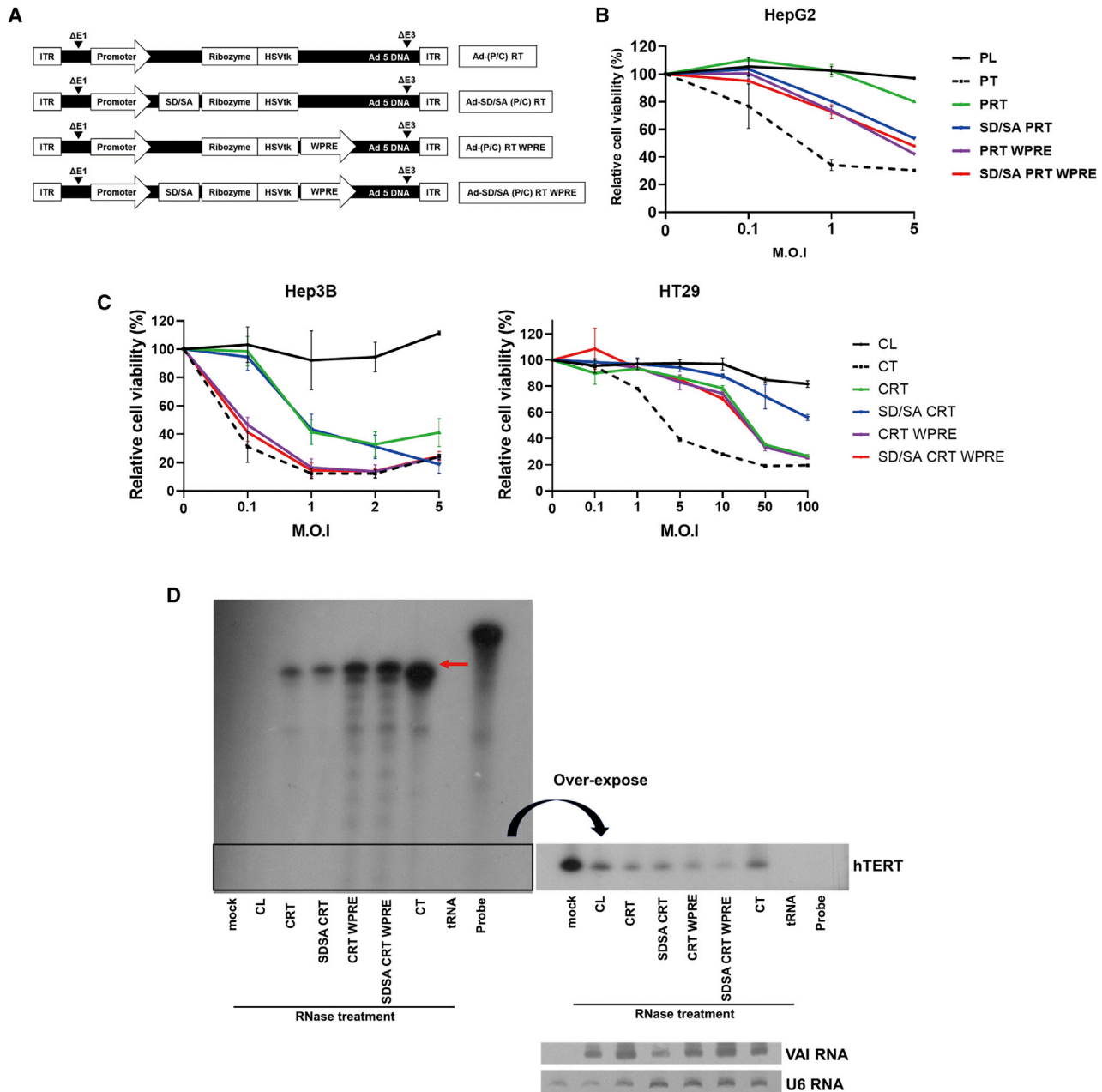


Figure 1. Comparison of the therapeutic efficacy of the enhancer element (SD/SA, WPRE, or both) containing adenoviral hTERT-specific *trans*-splicing ribozymes

(A) Schematic diagram of the enhancer element containing replication-incompetent adenoviral vectors with the Ad5 backbone and E1 and E3 deletion. (B and C) Efficacy of tumor cell-killing by the adenoviral vectors encoding ribozymes with enhancer element. HepG2 (B), Hep3B, and HT29 (C) cells were infected with each recombinant adenovirus at various MOI and treated with 100 μ M of GCV. Cell viability was determined by colorimetric method (MTS assay). Results are mean with SD of triplicate measurements. (D) Ribonuclease protection assay (RPA) was carried out in Hep3B cells to observe TSM by ribozymes with enhancer elements. Total RNA was extracted from cells infected by 10 MOI of each adenoviral vector and hybridized with the labeled TSM probe to detect *trans*-splicing molecules (red arrow) and hTERT RNA.

RNA reduction. Accordingly, modified ribozyme adenoviral vector harboring both SD/SA and WPRE was used for the following experiments.

Improved anti-HCC activity but higher hepatotoxicity *in vivo* by adenovirus harboring the post-transcriptionally enhanced *trans*-splicing ribozyme

Ad-PRT was observed to improve liver tissue specificity of the hTERT-targeting *trans*-splicing ribozyme,⁹ however, high titers of adenovirus are needed for *in vivo* delivery due to weak promoter activity. We tested whether the adenovirus encoding the ribozyme with enhancer SD/SA and WPRE (Ad-SD/SA PRT WPRE, Ad-EPRT) could regress HCC at a lower dosage, compared with Ad-PRT (Figures 2A and 2B). To this end, the adenovirus was systemically infected once into the intrahepatic multifocal mouse HCC xenograft model. Ad-PRT/GCV reduced ~90% of tumor weight at 1×10^{11} VP and ~60% of tumor weight at 1×10^{10} VP, whereas 0.25×10^{10} VP did not regress tumor weight at all. In contrast, Ad-EPRT/GCV at 1×10^{11} VP and 1×10^{10} VP reduced tumor weight to levels comparable with Ad-PRT at 1×10^{11} VP, indicating that 10-fold less modified Ad-EPRT was needed to induce HCC regression, compared with unmodified Ad-PRT. Additionally, Ad-PRT- and Ad-EPRT-treated mice were observed to have relatively lower liver toxicity than PBS-treated group, except at 1×10^{11} VP of Ad-EPRT, indicating higher hepatotoxicity by Ad-EPRT at high titers (Figure 2C). This hepatotoxicity at high Ad-EPRT dose was also seen in terms of both liver enzyme activity (Figure 2D) and histopathology (Figure 2E) in non-tumor bearing nude mice infected with the virus and followed by GCV. Liver tissue exhibited lobular inflammation, hepatocyte degeneration, and apoptosis in the mice. This toxicity for the high dose group was speculated as being due to excessive expression of ribozymes by enhancer elements. The results indicated that enhanced ribozyme adenoviral vector could efficiently reduce HCC at a lower titer; however, greater liver cancer-specificity would be needed for safe HCC therapy.

Improved and selective cytotoxicity of liver cancer cells by adenovirus harboring *trans*-splicing ribozyme under the control of both post-transcriptional enhancer elements and microRNA

Previously, we constructed a ribozyme adenoviral vector under the control of the PEPCK promoter and miR-122a through inserting miR-122a target site (miR-122T, Ad-PRT-122T) to improve liver cancer selectivity.¹¹ To construct a ribozyme adenoviral vector harboring high antitumor efficiency combined with liver cancer selectivity, we inserted miR-122T at the 3' untranslated region (UTR) of the enhanced ribozyme construct of Ad-EPRT, resulting in Ad-EPRT-122T (Figure 3A), and tested its cytotoxicity with GCV treatment in diverse liver cancer cells. Ad-EPRT-122T efficiently induced cytotoxicity of miR-122a-negative Hep3B cell at levels comparable with Ad-EPRT-mut 122T (Figure 3B). In contrast, Ad-EPRT-122T induced cytotoxicity of miR-122a-positive Huh-7 and Huh-7.5 cells at much lower levels than Ad-EPRT-mut122T, indicating regulated transgene expression by the

level of miR-122a in target cells. However, Ad-EPRT-122T exhibited more cytotoxicity toward such miR-122a-positive cells than Ad-PRT-122T, indicating transgene induction due to highly expressed RNA by the enhanced ribozyme compared with intracellular miR-122a level. Adenoviral vectors encoding the ribozyme induced no cell cytotoxicity of hTERT-negative SK-LU-1 cells, indicating the ribozyme exhibited target specificity (Figure 3C). We confirmed the miR-122a-regulated transgene expression of Ad-EPRT-122T in the established HepG2 cell lines that express miR-122a through the tetracycline-inducible system (Tet-on; Figure 3D). Ad-EPRT-122T induced HepG2 cell cytotoxicity without tetracycline, but no cell cytotoxicity was seen with tetracycline treatment. To further analyze the correlation between cell cytotoxicity and the level of miR-122a and ribozyme in cells infected with Ad-EPRT-122T, we performed tetracycline concentration-dependent cytotoxicity assays in the established Hep3B cell clones expressing miR-122a through Tet-on (Figure 3E; Figure S3). As the tetracycline concentration increased, cell viability increased only in the Ad-EPRT-122T-treated group. Correspondingly, the miR-122a copy number increased and ribozyme RNA level decreased in a manner that was tetracycline-dependent only in the Ad-EPRT-122T-treated group. In contrast, cell cytotoxicity was independent of both tetracycline concentration and miR-122a level in other adenovirus-treated groups. This result indicated that the enhanced ribozyme harboring miR-122T could selectively induce cytotoxicity of miR-122a-positive liver cancer cells, the efficiency of which depends on the level of ribozyme expression relative to miR-122a level, without compromising its cytotoxic efficacy in miR-122a-negative liver cancer cells.

Improved anti-HCC activity with least hepatotoxicity *in vivo* by adenovirus harboring the post-transcriptionally enhanced and miR-122a-regulated *trans*-splicing ribozyme

Systemic delivery of Ad-EPRT-122T followed by the administration of GCV efficiently and viral dose-dependently regressed HCC in Hep3B intrahepatic and multifocal mouse xenograft models with the least hepatotoxicity (Figures 4A and 4B). The mean tumor weight values (g) were as follows: 2.93 ± 1.42 for the control/GCV group, 0.38 ± 0.31 for the Ad-PRT-122T/GCV group (1×10^{11} VP), 0.11 ± 0.2 , 0.14 ± 0.14 , 0.21 ± 0.22 , and 0.71 ± 0.89 for the Ad-EPRT-122T/GCV group (1×10^{11} VP, 2×10^{10} VP, 1×10^{10} VP, and 0.5×10^{10} VP, respectively), indicating that 10-fold less Ad-EPRT-122T was needed to induce HCC regression, compared with unmodified Ad-PRT-122T. The anti-HCC efficacy by Ad-EPRT-122T was comparable to the effect mediated by Ad-EPRT when systemically introduced into the intrahepatic and multifocal HCC mouse xenograft (Figure 4C). It should be noticed that systemic introduction of Ad-EPRT-122T showed no hepatotoxicity even at the high dose of 1×10^{11} VP (Figure 4A) at which level, high hepatotoxicity was exhibited by Ad-EPRT. Correspondingly, no hepatotoxicity was seen in non-tumor bearing nude mice infected with Ad-EPRT-122T and followed by GCV, even at the high dose of 1×10^{11} VP (Figure 4D). These results indicated that enhanced ribozyme adenoviral vector with

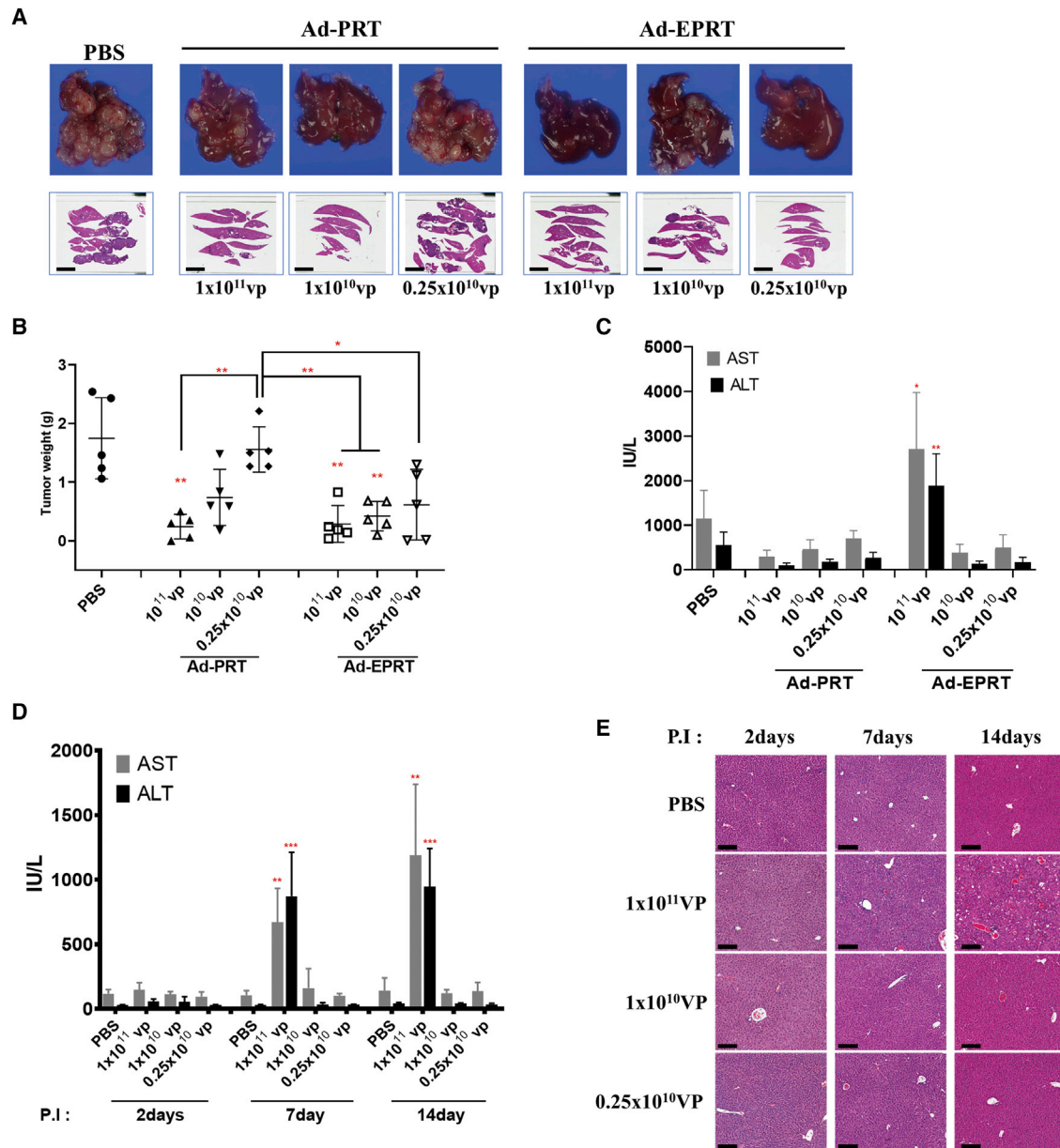


Figure 2. Enhanced anti-cancer efficacy but with high hepatotoxicity exhibited by Ad-EPRT in intrahepatic multifocal HCC model

(A) Representative gross (upper panel) and microscopic findings (lower panel) of entire livers in HCC-bearing mice systemically infected once with increasing titers of Ad-PRT or Ad-EPRT ($n = 5$ each) and followed by GCV treatment. The livers treated with each recombinant adenovirus were removed, serially sectioned, and embedded in paraffin block. The paraffin blocks were cut, and the tissue slides were stained with H&E and photographed under a virtual microscope. Microscopically, deep blue-colored nodules are HCC, and red-colored tissues are normal livers (scale bar, 5,000 μm). (B) Enhanced reduction of tumor weight by Ad-EPRT in mice of (A). Average tumor mass is presented with SD ($*p < 0.05$, $**p < 0.005$, Mann-Whitney test). (C) Liver enzyme levels of the virus and GCV-treated HCC-bearing mice of (A). Activity of liver enzymes, aspartate aminotransferase (AST) and alanine aminotransferase (ALT), was measured in serum by UV-spectrometer ($*p < 0.05$, $**p < 0.005$, unpaired t test). (D) Increasing titers of Ad-EPRT were systemically infected once together with GCV in non-tumor bearing normal mice. Five mice of each group were sacrificed at days 2, 7, and 14. Activity of liver enzyme in serum was measured by UV-spectrometer and is presented as means with SD ($**p < 0.005$, $***p < 0.0005$, unpaired t test). (E) Representative histology of liver treated with Ad-EPRT in mice of (D) (scale bar, 100 μm).

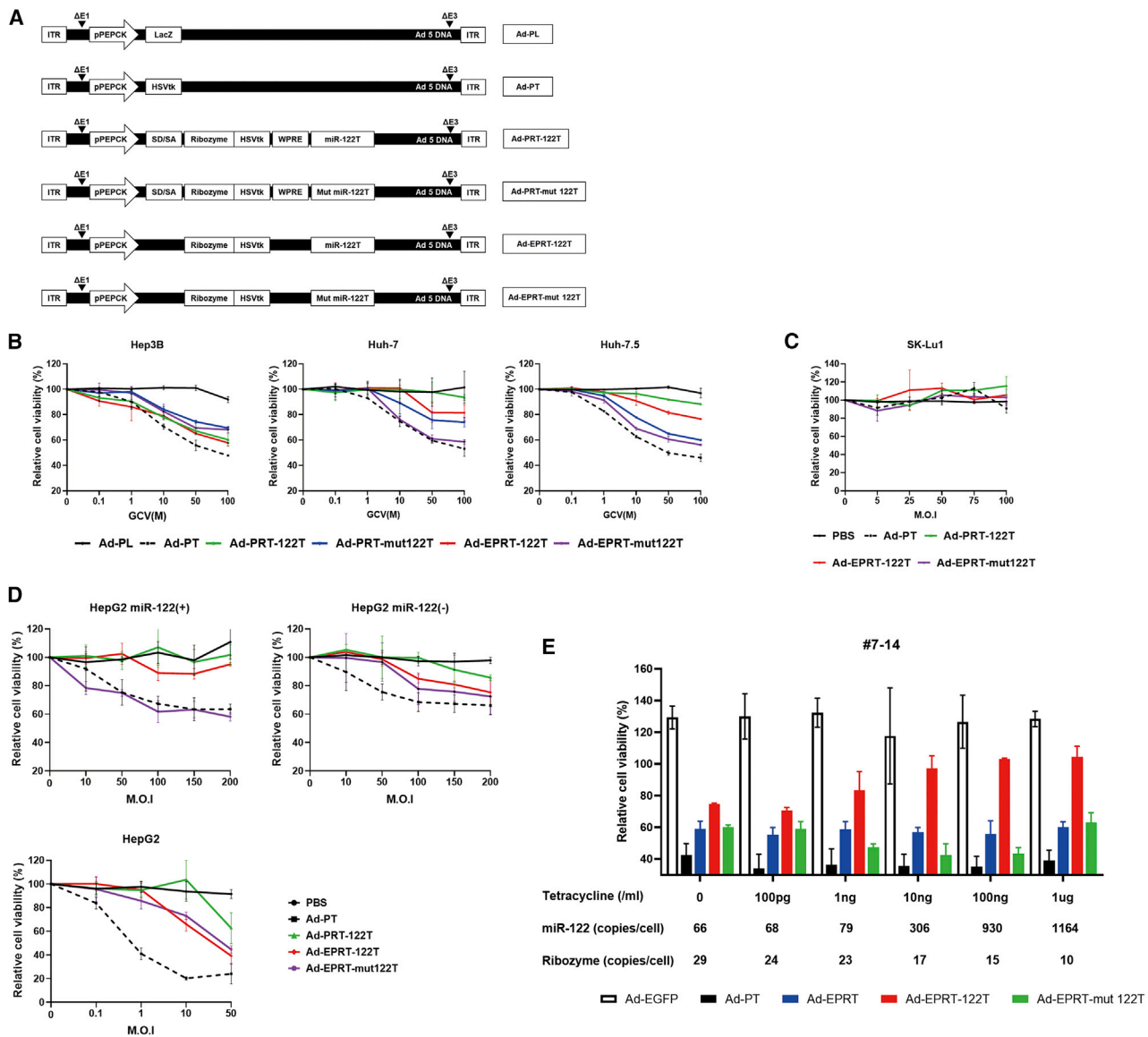


Figure 3. miR-122a-regulated hTERT-specific cytotoxicity and expression of Ad-EPRT-122T

(A) Schematic diagram of the refined adenoviral vector. (B) Selective cytotoxicity of the Ad-EPRT-122T according to miR-122a. Hep3B (miR-122a negative), Huh-7, and Huh-7.5 (miR-122a positive) cells were infected with each adenoviral vector at various MOI and treated with GCV. (C) SK-LU-1 cells (hTERT-negative) were infected with each adenovirus at various MOI and treated with GCV. (D) Original HepG2 and stable HepG2-Tet-on cells expressing miR-122a were infected with each adenoviral vector at various MOI and treated with GCV. (E) Cell viability was determined by MTS assay. Results are means \pm SD of triplicate measurements. (E) Each recombinant adenoviral vector (20 MOI) was transduced into stabilized Hep3B cell clone #7-14 having an miR-122a Tet-on system. Cell survival rate relative to PBS-treated sample and expression level of miR-122a and ribozyme were measured in each cell treated with the increasing concentrations of tetracycline.

miR-122a regulation could be used more safely than the adenoviral vector without miR-122a regulation and importantly, without compromising the efficacy of its anti-HCC effects.

Safe and improved anti-HCC efficacy, and expanded indications by CMV-driven ribozyme under the control of both post-transcriptional enhancer elements and microRNA

We constructed ubiquitously and highly active CMV promoter-driven hTERT targeting enhanced *trans*-splicing ribozymes, Ad-

ECRT and Ad-ECRT-122T, to test whether the ribozyme efficacy could be improved while maintaining minimal hepatotoxicity in diverse cancer types (Figure 5A). Ad-ECRT-122T efficiently induced cytotoxicity of miR-122a-negative liver cancer cells, SNU398, SNU449, and Hep3B, at levels comparable to Ad-ECRT, but with greater efficacy than Ad-EPRT or Ad-PRT-122T (Figure S4A). In contrast, Ad-ECRT-122T induced cytotoxicity of miR-122a-positive Huh-7 and Huh-7.5 cells to a lesser degree than Ad-ECRT, indicating its regulated transgene expression

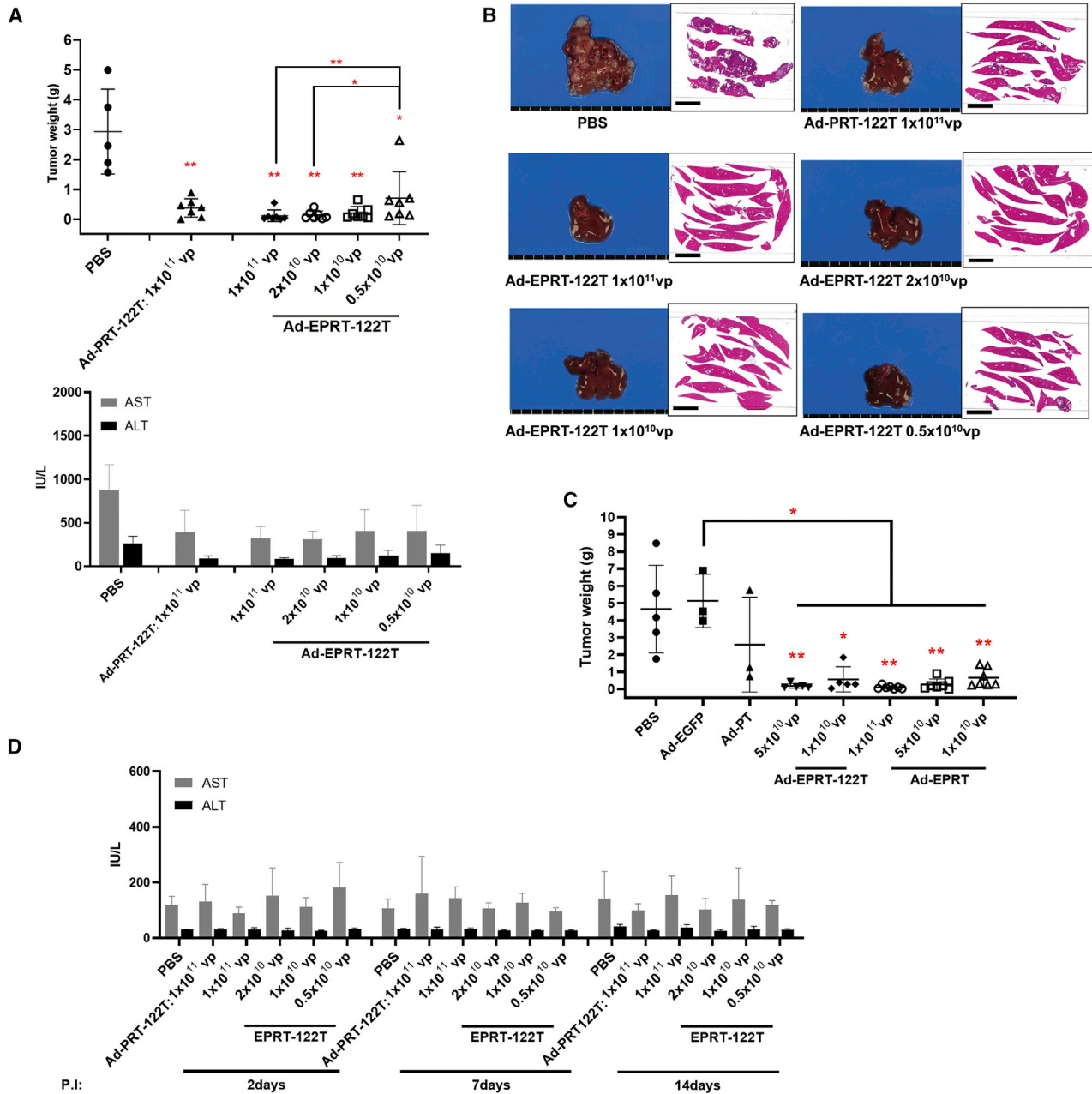


Figure 4. Anti-cancer efficacy and least hepatotoxicity of the Ad-EPRT-122T in intrahepatic multifocal HCC model

(A) Dose-dependent reduction of the tumor weight (upper panel; * $p < 0.05$, ** $p < 0.005$, Mann-Whitney test) and least liver toxicity (lower panel) by Ad-EPRT-122T. (B) Representative gross and microscopic findings of entire livers after treatment once with Ad-PRT-122T or various titers of Ad-EPRT-122T and GCV in HCC-bearing mice. The livers treated with each recombinant adenovirus were removed, serially sectioned, fixed, stained with H&E, and photographed under a virtual microscope (scale bar, 5,000 μm). (C) Comparison of anti-cancer efficacy in terms of reduction of tumor weights between Ad-EPRT and Ad-EPRT-122T (* $p < 0.05$, ** $p < 0.005$, Mann-Whitney test). (D) Ad-PRT-122T (1×10^{11} vp) or increasing titers of Ad-EPRT-122T were systemically infected once together with GCV in non-tumor bearing normal mice. Five mice of each group were sacrificed at days 2, 7, and 14. Activity of liver enzymes in serum was measured by UV-spectrometer and presented as means.

by miR-122a level in target cells. The ribozyme expression level in Ad-ECRT-122T-treated Huh-7.5 cells was lower than the level in the Ad-ECRT-treated cells at 10 multiplicities of infection (MOI) infection, confirming miR-122a-regulated gene expression by

Ad-ECRT-122T (Figure 5B). However, Ad-ECRT-122T exhibited greater cytotoxicity toward miR-122a-positive cells than Ad-EPRT-122T had, indicating transgene induction due to highly expressed RNA by the enhanced ribozyme (Figure S4A). In the miR-

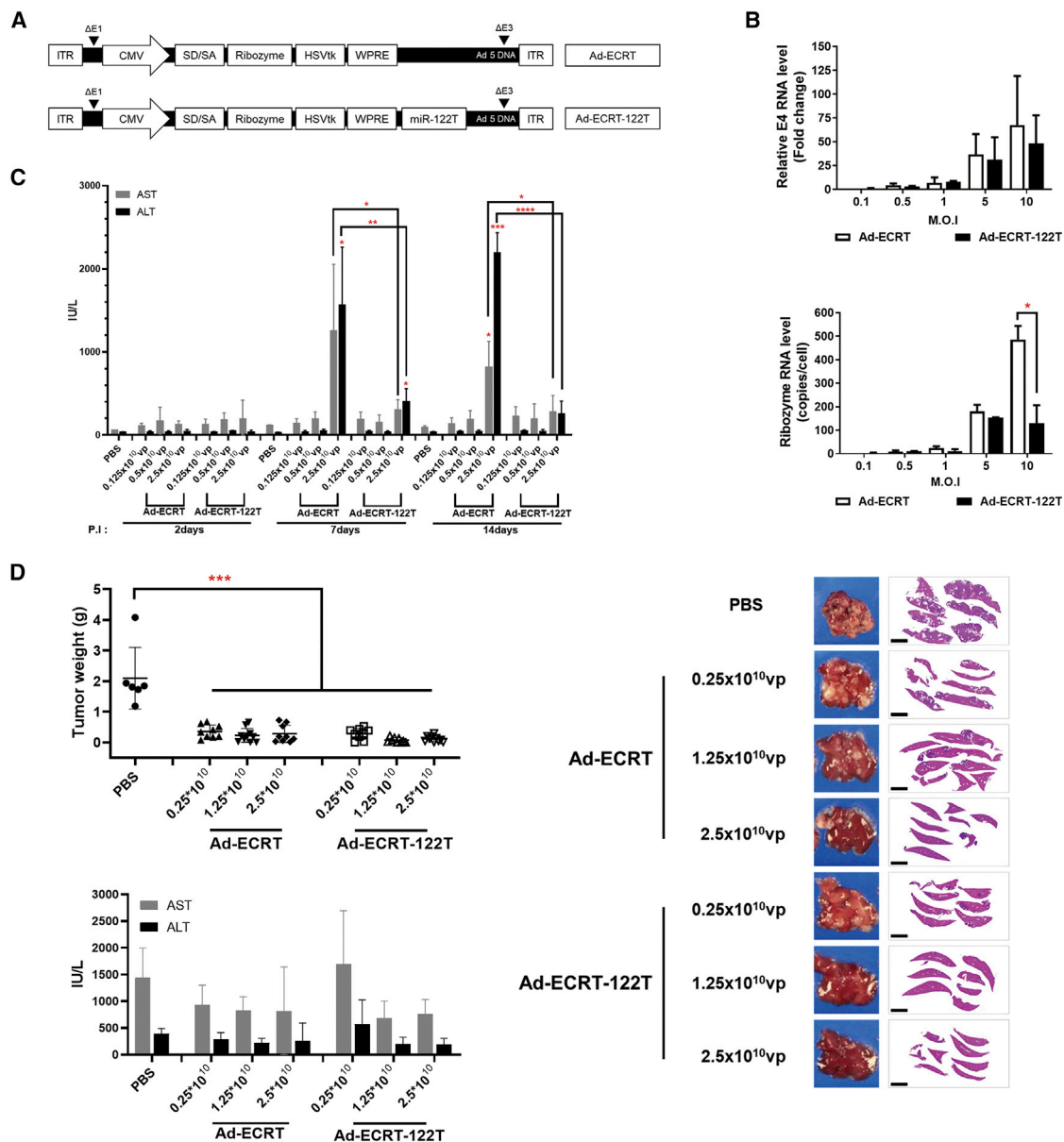


Figure 5. miR-122a-regulated expression of Ad-ECRT-122T and its anti-cancer efficacy in intrahepatic multifocal HCC model

(A) Schematic diagram of adenoviral vectors containing an expression cassette for a CMV promoter-based enhanced ribozyme. (B) RNA expression level of E4 (top panel) and ribozyme (bottom panel) in Huh-7.5 cell lines treated with increasing MOIs of Ad-ECRT or Ad-ECRT-122T. Data are presented as means with SD (* $p < 0.05$, unpaired t test). (C) Various amounts of Ad-ECRT or Ad-ECRT-122T were systemically infected once together with GCV in non-tumor bearing normal mice. Five mice of each group were sacrificed at days 2, 7, and 14. Activity of liver enzyme in serum was measured by UV-spectrometer and is presented as means with SD (* $p < 0.05$, ** $p < 0.005$, *** $p < 0.0005$, **** $p < 0.0001$, unpaired t test). (D) Comparison of anti-cancer efficacy (left upper panel) and liver toxicity (left lower panel) in HCC-bearing mice systemically infected once with increasing amount of Ad-ECRT or Ad-ECRT-122T and followed with GCV treatment. Representative gross findings of entire livers and H&E staining of the same tissues are presented in the adenovirus-treated HCC-bearing mice (right panel; scale bar, 5,000 μm). Tumor weight is shown as means with SD (** $p < 0.0005$, Mann-Whitney test).

122a-positive cells, the efficacy of Ad-ECRT-122T was comparable to the activity shown by Ad-CRT which was the originally constructed adenoviral vector encoding hTERT RNA-targeting ribozyme under a CMV promoter⁷ (Figure S4B).

Of note, high hepatotoxicity was shown in non-tumor bearing nude mice systemically infected with Ad-ECRT and followed by GCV at a

dose of 2.5×10^{10} VP, in contrast with Ad-ECRT-122T that induced relatively much lower hepatotoxicity even at the same dose (Figure 5C). This demonstrated the necessity of miR-122a-regulation for conferring minimal hepatotoxicity to add to the utility of the CMV promoter-driven enhanced ribozyme. Significant anti-HCC efficacy by Ad-ECRT-122T was shown at all tested dose from 2.5×10^9 to 2.5×10^{10} VP, with up to 86%–96% inhibition of tumor

growth. These levels were comparable to the effectiveness of Ad-ECRT, when systemically introduced once into the intrahepatic and multifocal HCC mouse xenograft and followed by GCV treatment (Figure 5D).

The anti-HCC efficacy of Ad-ECRT-122T was greater than seen with Ad-CRT-122T or Ad-EPRT in not only diverse liver cancer cells, but also the subcutaneous mouse HCC xenograft model (Figure S5). Vial dose-dependent anti-HCC effects were shown in the Ad-ECRT-122T/GCV treated mice (Figure S6). Moreover, Ad-ECRT-122T efficiently induced cytotoxicity in diverse telomerase-positive cancer types including colon cancer, glioblastoma, melanoma, cervical cancer, lung cancer, and breast cancer cells (Figure S7). This demonstrated that CMV promoter-driven enhanced ribozyme adenoviral vector with miR-122a regulation could be used safely and efficiently in diverse telomerase-expressing cancer cells. The *in vivo* availability of Ad-ECRT-122T in terms of single dose toxicity and tissue distribution was further assessed.

***In vivo* hepatotoxicity and tissue biodistribution of Ad-ECRT-122T**

Intravenous (i.v.) administration of Ad-ECRT-122T to normal mice at a single dose of 2.5×10^{10} VP produced minimal to mild increases in the liver enzyme level and microscopic changes in the liver (Figure 6A; Table S1). These effects were also seen in the livers of mice infected with the adenovirus combined with GCV treatment (Figure 6B; Table S2). In contrast, administration of Ad-ECRT-122T at single doses of 2.5×10^9 or 1.0×10^{10} VP produced least changes in the liver enzyme levels and microscopic features in the liver irrespective of GCV treatment. Based upon the absence of clinical pathology and the low incidence of findings in the liver, a no-observable-adverse-effect-level (NOAEL) of 1.0×10^{10} VP of Ad-ECRT-122T could be established for mice. Biodistribution of Ad-ECRT-122T administered by i.v. injection was analyzed in normal ICR mice at a single dose (2.5×10^{10} VP; Figure 6C). Liver was the major delivery target organ of the systemically injected Ad-ECRT-122T. The injected Ad-ECRT-122T had completely disappeared from blood by day 11 and beginning at 8 days after the systemic injection and within 2 weeks of the injection, 70% of ECRT-122T DNA had disappeared from the liver.

The hepatic artery is known to be the major route for supplying nutrients to primary HCC,^{23,24} implying that it would be an appropriate delivery route for introducing Ad-ECRT-122T. We tested *in vivo* biodistribution and hepatic expression of Ad-ECRT-122T administered into normal rats through hepatic artery at a single dose of 2.5×10^{11} VP (Figure S8A). The greatest amount of ECRT-122T DNA was detected in the liver on the second day after injection and 98% of the viral DNA had disappeared from the liver by day 14. Most of the viral DNA had also disappeared from other tissues including blood. Correspondingly, expression of ribozyme RNA in the liver of rats injected with Ad-ECRT-122T had almost completely disappeared by day 14 (Figure S8B). No changes in liver enzyme levels was shown in rats injected via hepatic artery at all administered titers (Figure S8C). These results

implied that i.v. or hepatic artery delivery could be safely and appropriately used for clinical application of Ad-ECRT-122T to HCC patients.

DISCUSSION

In this study, we developed group I intron-based and post-transcriptionally regulated *trans*-splicing ribozymes to induce therapeutic suicide gene activity. The aim was to efficiently and specifically target hTERT-expressing liver cancer at low delivery doses with minimal to no hepatotoxicity. To increase antitumor efficacy, we introduced post-transcriptionally enhancing elements including SD/SA and WPRE into the ribozyme expression construct. This resulted in increased intracellular expression of *trans*-splicing molecules with simultaneous reductions in the target hTERT RNA level, resulting in improved cytotoxicity. To increase liver cancer selectivity and minimize hepatotoxicity, we introduced target sites of miR-122a into the ribozyme expression cassette. miR-122a is the major miRNA in normal liver tissue^{22,25} and its level is highly repressed in most HCC.^{26–28} We verified improved anti-cancer effects and miRNA-regulated transgene expression in diverse hTERT-positive and miR-122a-positive/negative liver cancer cells. Moreover, *in vivo* efficacy and safety of the enhanced ribozymes was verified in the clinically relevant animal models, intra-hepatic and multifocal mouse HCC xenograft models.

For delivery of the ribozyme construct, recombinant adenovirus was used. Although the adenovirus offers efficient gene delivery for most tissues, especially liver cancer, its introduction into patients could induce innate immune responses, toxicity of viral proteins to normal tissues, and host-derived neutralizing antibodies, especially at high levels of adenovirus and thus its repeated introduction can be problematic.^{29–34} Moreover, the possibility of pre-existing anti-adenoviral antibodies in the patients could limit the number of patients that can be recruited for clinical trials. To overcome these limitations of the adenoviral vector for clinical studies, we tried to minimize both the number of injected doses and the amount of introduced virus. To this end, we tested the antitumor effects of the ribozyme adenoviral vector with just a single dose in all of *in vivo* experiments.

We enhanced ribozyme expression using post-transcriptionally enhancing elements and selected the most optimized version of ribozyme adenoviral vector that could efficiently induce anti-tumor effects with only a single dose and minimal virus amount in the HCC animal model. Under these criteria, Ad-ECRT-122T, which expresses CMV promoter-driven, post-transcriptionally enhanced, and regulated ribozyme under the control of SD/SA, WPRE sites, and miR-122a, was the most optimized reagent. We observed that more than 86% of HCC growth was retarded by systemic administration of a single dose of 2.5×10^9 VP of Ad-ECRT-122T. NOAEL of Ad-ECRT-122T was 1.0×10^{10} VP, 4-fold higher than the effective dose showing more than 86% anti-HCC efficacy, indicating the potentially clinical utility of Ad-ECRT-122T.

Another way to minimize the limitations associated with adenoviral vector for HCC therapy is to find the most appropriate delivery route

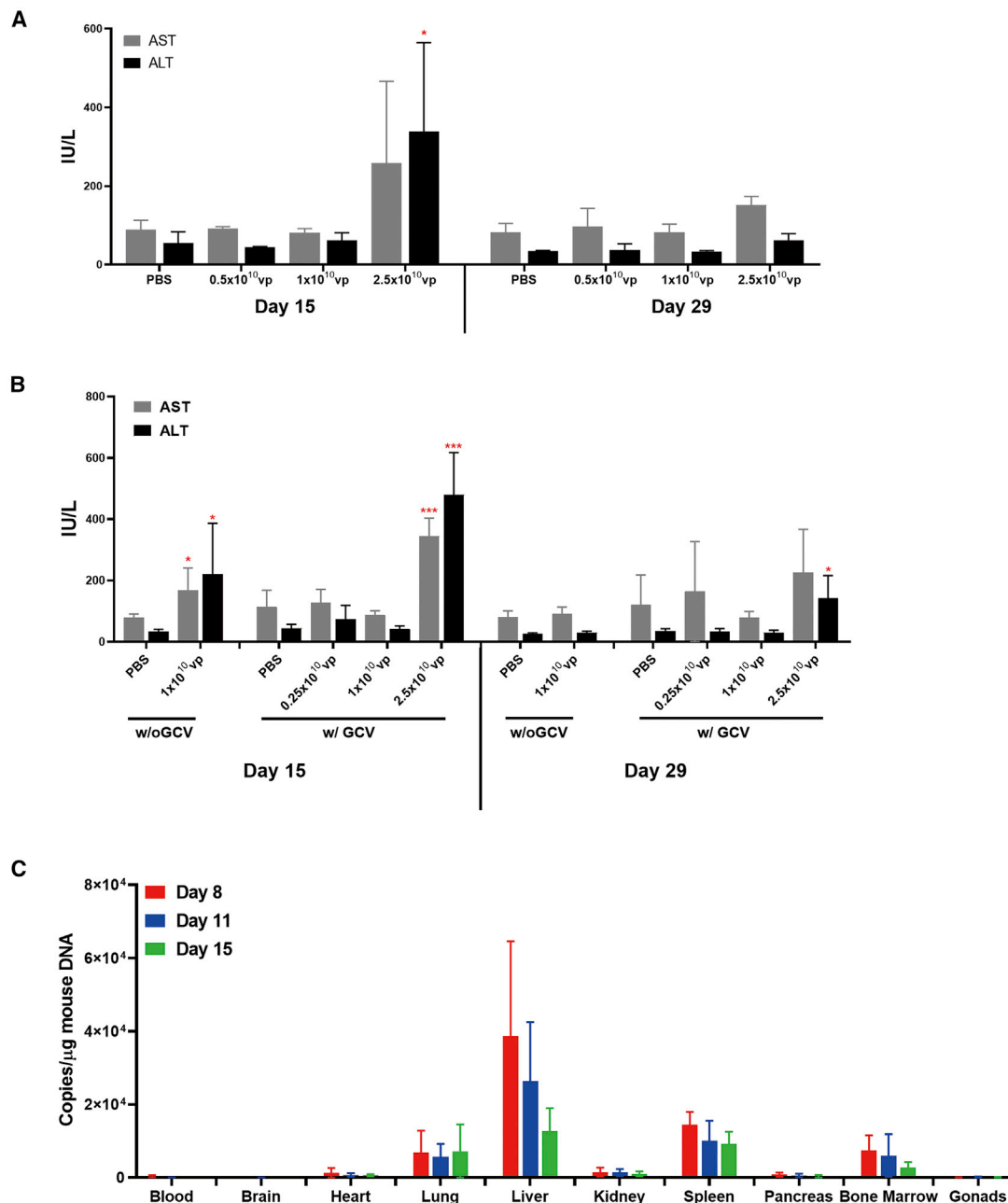


Figure 6. Liver enzyme activity and tissue biodistribution of Ad-ECRT-122T in normal ICR mice

(A and B) AST/ALT levels were measured over time (15 and 29 days after infection) with increasing amounts of Ad-ECRT-122T either without (A; n = 5) or with GCV treatment (B; n = 5; *p < 0.05, **p < 0.005, ***p < 0.0005, unpaired t test). (C) Amount of ribozyme DNA in each tissue was measured over time using qPCR after i.v. injection of Ad-ECRT-122T (2.5×10^{10} VP) in normal ICR mice (n = 10). All data are presented as means with SD.

for vector into patient. Most experiments presented here including efficacy and safety were performed by systemic delivery of the adenovirus through i.v. injection. More local introduction of the viral vector has been tried for HCC by introduction of the virus through hepatic artery.^{35–38} Accordingly, we verified the tissue distribution and clearance of Ad-ECRT-122T through hepatic artery injection as well and

observed no toxicity of the introduced virus in rats. Therefore, hepatic artery introduction of the ribozyme adenoviral vector could be an optimum delivery route for the introduction of the ribozyme adenoviral vector in clinical studies. To prove this, anti-HCC effects of the virus might need to be tested through hepatic artery introduction into intrahepatic and multifocal HCC animal model.

We assessed the availability of the miR-122a target site in terms of liver cancer selective cytotoxicity by analyzing correlations between the amount of ribozyme RNA and miRNA-122a with inducibility of cytotoxicity by the virus in liver cancer cells expressing miR-122a. Cytotoxicity of cells was observed when the copy number of miR-122a in cancer cells is less than approximately 100-fold the copy number of ribozymes expressed in the cells infected with the adenovirus. We analyzed miR-122a expression level in tissues of surgically resected HCC patients and observed much lower levels of miR-122a in liver cancer tissues in most patients with the exception of some of HCV-related ones, when compared with the level in normal liver (Figure S9). Moreover, the expression of miR-122a is relatively high in well differentiated tumors, but highly repressed in poorly differentiated, aggressive, and invasive HCCs.²⁸ Taken together, our enhanced and optimized ribozyme adenoviral vector could confer benefits to patients with advanced HCC, which is difficult to manage by current therapeutic approaches.

TERT-targeting *trans*-splicing ribozymes could be a multifunctional anticancer regimen due to TERT depletion and simultaneous cancer cell-specific induction of cytotoxicity.³⁹ This cumulative ribozyme activity could overcome the shortcomings of telomerase inhibition-only approaches, which suffer from the lag phase between the time of telomerase inhibition and the time of telomere shortening for conferring damage to cancer growth or the possibility of increased malignancy due to genomic instability.⁴⁰ The ribozyme-mediated depletion of TERT was shown to contribute to disruption of telomere integrity and DNA damage and to *in vivo* anti-tumor activity through suppression of metastasis- or angiogenesis-related pathways.⁴¹ Moreover, local and systemic immunity was induced by administration of ribozyme adenoviral vector followed by GCV treatment in a syngeneic mouse HCC model.¹¹ Recently, somatic mutations of TERT promoter have been found in several tumor types including HCC. TERT promoter mutations can increase the expression of telomerase transcripts and are one of earliest and the most frequent genetic alteration events in HCC.⁴² Of note, most cancer cells including HCC (~90%) express hTERT,⁴³ indicating that our hTERT RNA-targeting suicide approach could be applicable to genetically heterogeneous tumors. Indeed, CMV promoter-driven enhanced ribozyme was observed to efficiently hamper the growth of diverse types of cancer cells. Together with these multifunctional antitumor activities, the post-transcriptionally regulated hTERT-targeting ribozyme developed and optimized in this study in terms of anti-cancer efficacy and safety could be an effective therapeutic candidate against diverse human cancers including advanced HCC.

MATERIALS AND METHODS

Design of ribozyme expression construct

The hTERT-targeting ribozyme was designed to be directed at the +21 uridine residue of the hTERT RNA 5'-UTR and contained an extended internal guide sequence, including an extension of the P1 helix and an additional 6 nt-long P10 helix, and a 325-nt antisense sequence against the downstream region of the hTERT RNA target site.⁶ HSVtk cDNA was introduced as a 3' exon of the ribozyme.

SD/SA cDNA was inserted between CMV or PEPCK promoter and the antisense sequence. WPRE cDNA was inserted downstream of the HSVtk 3' exon. Three copies of the target site of miR-122a (122T, 5'-ACAAACACCATTGTCACACTCCA-3') or seed reverse sequence of miR-122a as a control (mut 122T, 5'-ACAAACACCA TTCCTCACACTGA-3') were inserted into the 3' UTR of the ribozyme expression construct.

Construction of recombinant adenoviral vectors

Expression vectors encoding the hTERT-specific ribozyme and HSVtk gene at the 3' exon with or without post-transcriptional regulators including enhancer elements (SA/SA and/or WPRE) and three copies of 122T under the control of the CMV or PEPCK promoter were cloned into the pAdenoVator-CMV5-IRES-GFP shuttle vector (Qbiogene, Irvine, CA, USA) to generate recombinant adenoviral vectors. Recombinant adenovirus vectors encoding the ribozymes were created by a homologous recombination technique in bacteria (BJ5183) as follows. In brief, the shuttle plasmid was linearized with PmeI and subsequently co-transformed into BJ5183 cells with an E1/E3 deleted adenoviral type5 backbone genome (pAdenoVator DE1/E3; Qbiogene). The recombinant vectors generated through homologous recombination in the bacteria were isolated and linearized with PacI. The linearized vectors were then transfected into HEK293 cells, and the recombinant adenoviruses produced were isolated by three rounds of plaque purification. Recombinant viruses were amplified, purified, qualified, and concentrated via ultracentrifugation (Beckman-Coulter, Brea, CA, USA). Titers of the recombinant adenovirus were determined by TCID50 analysis.

Cells

Hep3B, SNU182, SNU387, SNU398, SNU449, and PLC/PRF/5 (human hepatocellular carcinoma), HepG2 (human hepatoblastoma), SK-LU-1 and IMR90 (telomerase negative human lung carcinoma and normal lung fibroblast, respectively), NCI-H460 (human non-small cell lung carcinoma), HT29, HCT116, LS174T, SW480, and LOVO (human colorectal cancer), HEK293 (adenoviral E1-transformed human embryonic kidney cell line), LN229, T98G, and U87MG (human glioblastoma), HeLa (human cervical cancer), MCF7 (human breast cancer), and AGS (human gastric cancer) were purchased from the American Type Culture Collection (Manassas, VA, USA). Huh-7 and Huh-7.5 (human hepatoma) were obtained from the Japanese Collection of Research Bioresources Cell Bank (Osaka, Japan). Hs294T and SK-MEL2 (human melanoma) were purchased from the Korean Cell Line Bank (Seoul, Republic of Korea). Hep3B, HepG2, T98G, U87MG, SK-MEL2, HeLa, LS174T, and MCF-7 were cultured in MEM (Invitrogen, Carlsbad, CA, USA) with 10% FBS. SK-LU-1, Huh7, Huh-7.5, HT29, SW480, LN229, Hs294T, and HEK293 cells were maintained in DMEM (Invitrogen) with 10% FBS. SNU182, SNU387, SNU398, SNU449, PLC/PRF/5, HCT116, LOVO, AGS, IMR90, and NCI-H460 were cultured in RPMI (Invitrogen) with 10% FBS.

For establishment of cell lines stably expressing miR-122a dependent on the presence of tetracycline, Hep3B or HepG2 cells expressing Tet

repressor vector, pcDNA 6/TR (Invitrogen), were isolated with blasticidin for 2 weeks. The selected cells were transfected with vector encoding pri-miR-122a, which was cloned into the tetracycline response element vector, pcDNA 4/myc-His B (Invitrogen), and zeocin resistant colonies were isolated for 2 weeks.

Cytotoxicity assay

Cells were seeded at 1×10^4 cells per well in 96-well plates, incubated overnight, and infected with varying MOI of the recombinant adenoviruses. At 1-day post-infection (PI), 100 μ M of GCV (CymeveneVR, Roche, Basel, Switzerland) was added to each plate. The media containing GCV was replaced every 48 h for 5 days, and CellTiter 96 AQueous one solution reagent (Promega, Madison, WI, USA) in 100 μ L of medium was added to each well and incubated for 1–4 h at 37°C, based on the rate of color change. Cell viability was evaluated by determination of absorbance at 490 nm. Cell survivability after GCV treatment was quantitated as the fraction of the absorbance of cells without GCV treatment and represented as the percentage relative to that of uninfected cells.

RPA

Trans-splicing molecule (TSM) DNA was generated by PCR using primer set (HSVtk Forward: 5'-TAATACGACTCACTATAGGGA TGGCTTCGTACCCCTGCCAT-3', HSVtk Reverse: 5'-GTGAGGA CCGTCTATATAAACCCGCAGTAG-3', TSM Forward: 5'-TAA TACGACTCACTATAGGGCAGGCAGCGCTGCGTCCT-3', TSM Reverse: 5'-GTGAGGACCGTCTATATAAACCCGCAGTAG-3') for DNA template. Amplified DNA was cloned into pJET 1.2/blunt vector (Fermentas, Waltham, MA, USA), linearized with XbaI, and run-off *in vitro* transcribed with T7 RNA polymerase and ³²P-UTP (Perkin Elmer, Waltham, MA, USA) to generate a radiolabeled RNA probe for TSM product. For RPA, recombinant adenovirus (10 MOI) was infected into Hep3B cells and total RNA was extracted after 48 h PI. Total RNA (30 μ g) was hybridized in 1 \times hybridization buffer (40 mM HEPES, 400 mM NaCl, 1 mM EDTA, deionized formamide, 80% v/v) with radiolabeled-RNA probe (5 fmoles) overnight at 45°C. Subsequently, 5 μ g RNase A and 10 U RNase T1 were added in RNase digestion buffer (10 mM Tris-Cl, 5 mM EDTA, 300 mM NaOAc, pH 7.5) to remove non-hybridized RNA, and proteinase K and SDS were added to remove RNase. Hybridized RNA was recovered with phenol treatment and ethanol precipitation and separated on a 10% denaturing acrylamide gel. The separated RNAs were visualized on X-ray film. As internal controls, VAI and U6 snRNA were detected by Northern blot analysis, according to the manufacturer's protocol (BrightStar BioDetect, Ambion, Austin, TX, USA), with biotinylated single-strand DNA oligonucleotide probe as follows: VAI probe: 5'-biotin-AAAAGGAGCGCTCCCCCGTTGTCTGACGTGCGACA CC-3', U6 probe: 5'-biotin-GAATTTGCGTGTATCCTTGCACA GGGGCCATGCTAA-3'.

RNA analysis in cells

Total RNA was extracted using Trizol (Invitrogen) from cells infected with recombinant adenovirus. cDNA was then synthesized by reverse transcription with a random hexamer or mature miR-122a probe

(Applied Biosystems, Waltham, MA, USA). For the calculation of *trans*-splicing ribozyme copy number, 2 μ L of the synthesized cDNA was subjected to qPCR with primers (5'-TTCCGGAGGACA GACACATCGA-3' and 5'-GCAGATACCGCACCGTATTGGC-3') at 95°C for 30 s, 58°C for 30 s, and 72°C for 30 s, for 40 cycles. For the calculation of miR-122a copy number, 2 μ L of the synthesized cDNA was mixed in 2 \times TaqMan Universal PCR Master Mix II with miR-122a TaqMan probe (Assay ID: 002245, Applied Biosystems). For adenoviral E4 gene amplification, 2 μ L of the synthesized cDNA was subjected to qPCR with primers (5'-GCTGG CAAAACCTGCCCGCCGGCTATA-3' and 5'-GCTCTAGATGG GTTGTTCCTGGGATATGGTT-3') at 95°C for 30 s, 58°C for 30 s, and 72°C for 30 s, for 40 cycles. qPCR was performed using StepOne Plus Real-time PCR instrument (Applied Biosystems).

In vivo anti-cancer efficacy

Male BALB/CAAn/CriBg-nu/nu nude mice (4 to 5 weeks old; NARA Bio, Seoul, Republic of Korea) were used. All procedures were authorized and approved by the Dong-A University College of Medicine ethics committee (project license no. DIACUC-19-12). The animals were kept under specific pathogen-free conditions and maintained in the Korean Food and Drug Administration animal facility in accordance with the AAALAC International Animal Care policy (accredited unit-Korea Food and Drug Administration: unit number: 000996). A mouse model of intrahepatic multifocal HCC was established by a modification of the splenic subcapsular inoculation of Hep3B cells previously described.¹¹ A linear incision of the left flank abdominal wall was made to visualize the spleen, and 3×10^6 cells in 100 μ L of PBS were injected under the spleen capsule with a 29-gauge needle. The injection site was pressed with an aseptic cotton sponge for several min to prevent further leakage, after which the abdominal wall was sutured with silk. The mice showed multiple tiny tumor nodules along the liver margin, easily detectable by gross inspection, on the 11th or 12th day. On the 12th day, various adenoviruses encoding *trans*-splicing ribozyme, and adenovirus encoding HSVtk gene without ribozyme under the control of CMV or PEPCK promoter (Ad-CT and Ad-PT, respectively) and PBS as controls were administered once via tail vein, followed by intraperitoneal injection of GCV at 50 mg/kg, twice daily for 10 days from the day after virus injection. On the day following the last GCV treatment, blood sampling through the heart for liver enzyme analysis (ALT or AST) was carried out. Liver enzymes were measured by the Automated Blood Chemistry Line (Toshiba 200 FR, Tokyo, Japan). All mice were euthanized, and the whole liver lobes were removed, measured, photographed, and serially sectioned in 2 mm thickness. Entire liver slices from each mouse were fixed in 10% neutralized buffered formalin and processed for paraffin embedding. Tissue sections of 4- to 6- μ m thickness were stained with hematoxylin and eosin (H&E) for morphologic examination. The microscopic images were scanned under virtual microscope (AperioTechnologica, Vista, CA, USA). The tumor fraction was calculated using the AperioImageScope program v10.2.2.2319, and the tumor weight was estimated by multiplication of liver weight and tumor fraction.

Alternatively, BALB/C nude mice (6 weeks old; OrientBio, Seongnam, Republic of Korea) were used for subcutaneous mouse xenograft. SNU398 cells (5×10^6) were inoculated subcutaneously in the right flank of mice. When the mean tumor volume reached 100 mm^3 after tumor cell inoculation, mice of each group were injected twice for 2 days with the recombinant adenovirus (1×10^9 viral particle, VP) encoding *trans*-splicing ribozyme via intratumoral injection, followed by intraperitoneal injection of GCV at 50 mg/kg, twice daily for 10 days from the day after first virus injection. Anti-tumor efficacy was evaluated according to the tumor growth inhibition relative to the control adenovirus (Ad-EGFP).

***In vivo* toxicity**

***i.v.* injection**

Ad-ECRT-122T was *i.v.* injected once, either with, or without GCV, into normal ICR mice (SAMTAKO Bio Korea, Osan, Republic of Korea) at various doses. On day 15 and 29 after the injection, AST and ALT levels were measured. After the virus injection, orbital blood collection was performed on day 15 using a capillary tube (Kimble Chase, Vineland, NJ, USA), and at the end of the test period (day 29), CO₂ inhalation anesthesia was performed, and cardiac blood collection was performed using a disposable syringe (1 mL, 26G1/2"). The blood was coagulated by standing at room temperature for 20 min and then centrifuged for 10 min. AST/ALT levels were determined using a blood biochemical analyzer (Chemistry Analyzer, AU480, Beckman-Coulter). All blood was collected in a non-fasted state.

Hepatic artery injection

Ad-ECRT-122T was injected once into Sprague Dawley (SD) rats (OrientBio) by hepatic artery injection as follows. SD rats were opened under respiratory anesthesia with isoflurane, and then the liver and blood vessels were exposed to separate the gastroduodenal artery. After separation, the adenovirus was carefully administered with a 0.3 mL syringe while identifying the location of the blood vessel under a microscope. After administration, the abdominal wall was closed with a simple nodule with an absorbable suture, and the skin was closed with a suture clip. At 15 and 29 days PI, blood was collected from the jugular vein on each blood collection day. The AST/ALT levels were determined as described in *i.v.* injection.

***In vivo* distribution**

***i.v.* injection**

Ad-ECRT-122T was injected into normal ICR mice at a dose of 2.5×10^{10} VP by *i.v.* injection, and then, 8, 11 and 15 days later, each major organ was isolated to extract DNA. The extracted DNA was subjected to real-time PCR at 95°C for 15 s and 60°C for 60 s, for 40 cycles using 7500 FAST Real-Time PCR system (Applied Biosystems) using primer sets to analyze Ad-ECRT-122T distribution in major tissues using the following oligonucleotides; Forward: 5'-GGCCTTGCAAAGGGTATGG-3', Reverse: 5'-TAGGACTTGGCTGCGTGGTT-3' and probe (FAM): 5'-AATAAGCTGACGGACATGG [MGB]-3'.

Hepatic artery injection

Ad-ECRT-122T was injected into SD rats at a dose of 2.5×10^{11} VP by hepatic artery injection as described in *in vivo* toxicity analysis, and then, 2 and 14 days later, each major organ was isolated to extract DNA. Ad-ECRT-122T distribution was analyzed by the same method for *i.v.* injection. For RNA analysis, total RNA was extracted from liver tissue using Trizol. cDNA was synthesized by reverse transcription with Oligo-dT primer using a ReverTra Ace reverse transcriptase (Toyobo, Dublin, OH) and 2 μL of the synthesized cDNA was subjected to qPCR at 95°C for 15 s and 60°C for 60 s, for 40 cycles with PCR primers used in the *i.v.* injection method using ViiA7 real-time PCR instrument (Applied Biosystems).

miR-122a RNA analysis in HCC patient tissue

miR-122a expression was analyzed in tissues from 70 HCC patients obtained from the Bio-Resource Bank at Dong-A University Medical Center in Korea (IRB no. DKU2017-05-003-002). Total RNA from a normal liver tissue sample and a liver cancer tissue sample from each liver cancer patient was extracted using Trizol. cDNA was synthesized by reverse transcription from 50 ng of extracted RNA using a TaqMan Reverse Transcription kit, and 1 μL of the synthesized cDNA was mixed with a TaqMan 2 \times Universal PCR Master Mix and subjected to PCR using a StepOne Plus instrument (Applied Biosystems). PCR was performed using a TaqMan probe provided by ABI (Assay ID:002245, Applied Biosystems).

SUPPLEMENTAL INFORMATION

Supplemental Information can be found online at <https://doi.org/10.1016/j.omtn.2020.10.036>.

ACKNOWLEDGMENTS

This work was supported by Business for Startup Growth and Technological Development (TIPS Program) funded by Korea Small and Medium Business Administration in 2017 (grant no. S2566697) and by the National Research Foundation of Korea (NRF, Republic of Korea) funded by the Ministry of Science and ICT (2017M3A9C8031781, 2019M3E5D5065771, and 2020M3A9C8017745). We thank to Drs. Soohan Lee and Hyo-Young Chung at Osong Medical Innovation Center and Dr. Myeong-Mi Lee at Chungbuk National University for their contributions to the biodistribution study in mice and rats and liver toxicity study in rats.

AUTHOR CONTRIBUTIONS

S.-W.L. and J.S.J. designed the experiments; S.R.H., C.H.L., J.Y.L., J.H.K., J.H.K., S.J.K., Y.W.C., E.K., Y.K., J.-H.R., and M.H.J. conducted the experiments; and S.R.H., C.H.L., J.S.J., and S.-W.L. analyzed data and wrote the manuscript.

DECLARATION OF INTERESTS

S.R.H. and J.H.K. are employee of Rznomics. J.S.J. is a stockholder of Rznomics. S.-W.L. is CEO of Rznomics. No potential conflicts of interest were disclosed for other authors.

REFERENCES

- El-Serag, H.B., and Rudolph, K.L. (2007). Hepatocellular carcinoma: epidemiology and molecular carcinogenesis. *Gastroenterology* 132, 2557–2576.
- Yang, J.D., Hainaut, P., Gores, G.J., Amadou, A., Plymoth, A., and Roberts, L.R. (2019). A global view of hepatocellular carcinoma: trends, risk, prevention and management. *Nat. Rev. Gastroenterol. Hepatol.* 16, 589–604.
- Faloppi, L., Scartozzi, M., Maccaroni, E., Di Pietro Paolo, M., Berardi, R., Del Prete, M., and Cascinu, S. (2011). Evolving strategies for the treatment of hepatocellular carcinoma: from clinical-guided to molecularly-tailored therapeutic options. *Cancer Treat. Rev.* 37, 169–177.
- Global Burden of Disease Cancer Collaboration, Fitzmaurice, C., Allen, C., Barber, R.M., Barregard, L., Bhutta, Z.A., Brenner, H., Dicker, D., Chimed-Orchir, O., Dandona, R., Dandona, L., et al. (2017). Global, regional, and national cancer incidence, mortality, years of life lost, years lived with disability, and disability-adjusted life-years for 32 cancer groups, 1990 to 2015: a systematic analysis for the global burden of disease study. *JAMA Oncol.* 3, 524–548.
- McCormick, F. (2001). Cancer gene therapy: fringe or cutting edge? *Nat. Rev. Cancer* 1, 130–141.
- Kwon, B.S., Jung, H.S., Song, M.S., Cho, K.S., Kim, S.C., Kimm, K., Jeong, J.S., Kim, I.H., and Lee, S.W. (2005). Specific regression of human cancer cells by ribozyme-mediated targeted replacement of tumor-specific transcript. *Mol. Ther.* 12, 824–834.
- Hong, S.H., Jeong, J.S., Lee, Y.J., Jung, H.I., Cho, K.S., Kim, C.M., Kwon, B.S., Sullenger, B.A., Lee, S.W., and Kim, I.H. (2008). In vivo reprogramming of hTERT by trans-splicing ribozyme to target tumor cells. *Mol. Ther.* 16, 74–80.
- Jeong, J.S., Lee, S.W., Hong, S.H., Lee, Y.J., Jung, H.I., Cho, K.S., Seo, H.H., Lee, S.J., Park, S., Song, M.S., et al. (2008). Antitumor effects of systemically delivered adenovirus harboring trans-splicing ribozyme in intrahepatic colon cancer mouse model. *Clin. Cancer Res.* 14, 281–290.
- Song, M.S., Jeong, J.S., Ban, G., Lee, J.H., Won, Y.S., Cho, K.S., Kim, I.H., and Lee, S.W. (2009). Validation of tissue-specific promoter-driven tumor-targeting trans-splicing ribozyme system as a multifunctional cancer gene therapy device in vivo. *Cancer Gene Ther.* 16, 113–125.
- Won, Y.S., Jeong, J.S., Kim, S.J., Ju, M.H., and Lee, S.W. (2015). Targeted anticancer effect through microRNA-181a regulated tumor-specific hTERT replacement. *Cancer Lett.* 356 (2 Pt B), 918–928.
- Kim, J., Won, R., Ban, G., Ju, M.H., Cho, K.S., Young Han, S., Jeong, J.S., and Lee, S.W. (2015). Targeted regression of hepatocellular carcinoma by cancer-specific RNA replacement through microRNA regulation. *Sci. Rep.* 5, 12315.
- Wu, L., Johnson, M., and Sato, M. (2003). Transcriptionally targeted gene therapy to detect and treat cancer. *Trends Mol. Med.* 9, 421–429.
- Lechel, A., Manns, M.P., and Rudolph, K.L. (2004). Telomeres and telomerase: new targets for the treatment of liver cirrhosis and hepatocellular carcinoma. *J. Hepatol.* 41, 491–497.
- Kwon, B.S., Jeong, J.S., Won, Y.S., Lee, C.H., Yoon, K.S., Hyung Jung, M., Kim, I.H., and Lee, S.W. (2011). Intracellular efficacy of tumor-targeting group I intron-based trans-splicing ribozyme. *J. Gene Med.* 13, 89–100.
- Lacy-Hulbert, A., Thomas, R., Li, X.P., Lilley, C.E., Coffin, R.S., and Roes, J. (2001). Interruption of coding sequences by heterologous introns can enhance the functional expression of recombinant genes. *Gene Ther.* 8, 649–653.
- Nott, A., Meislin, S.H., and Moore, M.J. (2003). A quantitative analysis of intron effects on mammalian gene expression. *RNA* 9, 607–617.
- Furger, A., O'Sullivan, J.M., Binnie, A., Lee, B.A., and Proudfoot, N.J. (2002). Promoter proximal splice sites enhance transcription. *Genes Dev.* 16, 2792–2799.
- Donello, J.E., Loeb, J.E., and Hope, T.J. (1998). Woodchuck hepatitis virus contains a tripartite posttranscriptional regulatory element. *J. Virol.* 72, 5085–5092.
- Zufferey, R., Donello, J.E., Trono, D., and Hope, T.J. (1999). Woodchuck hepatitis virus posttranscriptional regulatory element enhances expression of transgenes delivered by retroviral vectors. *J. Virol.* 73, 2886–2892.
- Xu, Z.L., Mizuguchi, H., Mayumi, T., and Hayakawa, T. (2003). Woodchuck hepatitis virus post-transcriptional regulation element enhances transgene expression from adenovirus vectors. *Biochim. Biophys. Acta* 1621, 266–271.
- Loeb, J.E., Cordier, W.S., Harris, M.E., Weitzman, M.D., and Hope, T.J. (1999). Enhanced expression of transgenes from adeno-associated virus vectors with the woodchuck hepatitis virus posttranscriptional regulatory element: implications for gene therapy. *Hum. Gene Ther.* 10, 2295–2305.
- Lagos-Quintana, M., Rauhut, R., Yalcin, A., Meyer, J., Lendeckel, W., and Tuschl, T. (2002). Identification of tissue-specific microRNAs from mouse. *Curr. Biol.* 12, 735–739.
- Ackerman, N.B. (1974). The blood supply of experimental liver metastases. IV. Changes in vascularity with increasing tumor growth. *Surgery* 75, 589–596.
- Duan, F., and Lam, M.G.E.H. (2013). Delivery approaches of gene therapy in hepatocellular carcinoma. *Anticancer Res.* 33, 4711–4718.
- Chang, J., Nicolas, E., Marks, D., Sander, C., Lerro, A., Buendia, M.A., Xu, C., Mason, W.S., Moloshok, T., Bort, R., et al. (2004). miR-122, a mammalian liver-specific microRNA, is processed from hcr mRNA and may downregulate the high affinity cationic amino acid transporter CAT-1. *RNA Biol.* 1, 106–113.
- Gramantieri, L., Ferracin, M., Fornari, F., Veronese, A., Sabbioni, S., Liu, C.G., Calin, G.A., Giovannini, C., Ferrazzi, E., Grazi, G.L., et al. (2007). Cyclin G1 is a target of miR-122a, a microRNA frequently down-regulated in human hepatocellular carcinoma. *Cancer Res.* 67, 6092–6099.
- Tsai, W.C., Hsu, P.W.C., Lai, T.C., Chau, G.Y., Lin, C.W., Chen, C.M., Lin, C.D., Liao, Y.L., Wang, J.L., Chau, Y.P., et al. (2009). MicroRNA-122, a tumor suppressor microRNA that regulates intrahepatic metastasis of hepatocellular carcinoma. *Hepatology* 49, 1571–1582.
- Coulouarn, C., Factor, V.M., Andersen, J.B., Durkin, M.E., and Thorgeirsson, S.S. (2009). Loss of miR-122 expression in liver cancer correlates with suppression of the hepatic phenotype and gain of metastatic properties. *Oncogene* 28, 3526–3536.
- Juillard, V., Villefroy, P., Godfrin, D., Pavirani, A., Venet, A., and Guillet, J.G. (1995). Long-term humoral and cellular immunity induced by a single immunization with replication-defective adenovirus recombinant vector. *Eur. J. Immunol.* 25, 3467–3473.
- Worgall, S., Wolff, G., Falck-Pedersen, E., and Crystal, R.G. (1997). Innate immune mechanisms dominate elimination of adenoviral vectors following in vivo administration. *Hum. Gene Ther.* 8, 37–44.
- Otake, K., Ennist, D.L., Harrod, K., and Trapnell, B.C. (1998). Nonspecific inflammation inhibits adenovirus-mediated pulmonary gene transfer and expression independent of specific acquired immune responses. *Hum. Gene Ther.* 9, 2207–2222.
- Thomas, C.E., Birkett, D., Anozie, I., Castro, M.G., and Lowenstein, P.R. (2001). Acute direct adenoviral vector cytotoxicity and chronic, but not acute, inflammatory responses correlate with decreased vector-mediated transgene expression in the brain. *Mol. Ther.* 3, 36–46.
- Hartman, Z.C., Appledorn, D.M., and Amalfitano, A. (2008). Adenovirus vector induced innate immune responses: impact upon efficacy and toxicity in gene therapy and vaccine applications. *Virus Res.* 132, 1–14.
- Larocca, C., and Schlom, J. (2011). Viral vector-based therapeutic cancer vaccines. *Cancer J.* 17, 359–371.
- Carpenter, S.G., Carson, J., and Fong, Y. (2010). Regional liver therapy using oncolytic virus to target hepatic colorectal metastases. *Semin. Oncol.* 37, 160–169.
- Lin, X.J., Li, Q.J., Lao, X.M., Yang, H., and Li, S.P. (2015). Transarterial injection of recombinant human type-5 adenovirus H101 in combination with transarterial chemoembolization (TACE) improves overall and progressive-free survival in resectable hepatocellular carcinoma (HCC). *BMC Cancer* 15, 707.
- Altomonte, J., Muñoz-Álvarez, K.A., Shinozaki, K., Baumgartner, C., Kaissis, G., Braren, R., and Ebert, O. (2016). Transarterial administration of oncolytic viruses for locoregional therapy of orthotopic HCC in rats. *J. Vis. Exp.* 110, 53757.

38. Cho, E., Ryu, E.J., Jiang, F., Jeon, U.B., Cho, M., Kim, C.H., Kim, M., Kim, N.D., and Hwang, T.H. (2018). Preclinical safety evaluation of hepatic arterial infusion of oncolytic poxvirus. *Drug Des. Devel. Ther.* *12*, 2467–2474.
39. Lee, C.H., Han, S.R., and Lee, S.W. (2018). Therapeutic applications of group I intron-based trans-splicing ribozymes. *Wiley Interdiscip. Rev. RNA* *9*, e1466.
40. Hackett, J.A., and Greider, C.W. (2002). Balancing instability: dual roles for telomerase and telomere dysfunction in tumorigenesis. *Oncogene* *21*, 619–626.
41. Kim, Y.H., Kim, K.T., Lee, S.J., Hong, S.H., Moon, J.Y., Yoon, E.K., Kim, S., Kim, E.O., Kang, S.H., Kim, S.K., et al. (2016). Image-aided suicide gene therapy utilizing multi-functional hTERT-targeting adenovirus for clinical translation in hepatocellular carcinoma. *Theranostics* *6*, 357–368.
42. Nault, J.C., Mallet, M., Pilati, C., Calderaro, J., Bioulac-Sage, P., Laurent, C., Laurent, A., Cherqui, D., Balabaud, C., and Zucman-Rossi, J. (2013). High frequency of telomerase reverse-transcriptase promoter somatic mutations in hepatocellular carcinoma and preneoplastic lesions. *Nat. Commun.* *4*, 2218.
43. Nagao, K., Tomimatsu, M., Endo, H., Hisatomi, H., and Hikiji, K. (1999). Telomerase reverse transcriptase mRNA expression and telomerase activity in hepatocellular carcinoma. *J. Gastroenterol.* *34*, 83–87.